

Supporting Information for “Winter-Summer Contrast in the Response of Northern Hemisphere Precipitation Extremes to Climate Change”

Andrew Williams¹ and Paul A. O’Gorman²

¹Atmospheric, Oceanic and Planetary Physics, Department of Physics, University of Oxford, Oxford, UK

²Department of Earth, Atmospheric and Planetary Sciences, Massachusetts Institute of Technology, Cambridge, MA, USA

Contents of this file

Text S1 and Figures S1-S10.

Introduction

This document provides supporting text and figures for the main article.

1. Text S1 describes the CMIP5 models used in this study.
2. Figures S1-S10 support the findings in the main text.

Corresponding author: A. Williams, Department of Atmospheric, Oceanic and Planetary Physics, Department of Physics, University of Oxford, Oxford, UK. (andrew.williams@physics.ox.ac.uk)

Text S1.

We use the following 18 CMIP5 models: ACCESS1-0, ACCESS1-3, BNU-ESM, CMCC-CESM, CMCC-CM, CMCC-CMS, CNRM-CM5, CSIRO-Mk3-6-0, CanESM2, FGOALS-g2, GFDL-ESM2M, IPSL-CM5A-LR, IPSL-CM5A-MR, IPSL-CM5B-LR, MPI-ESM-LR, MPI-ESM-MR, NorESM1-M, bcc-csm1-1-m.

However, Figure 3 and Figures S5, S6 and S7 required RH_{2m} ('hurs') which was only available for the following 12 CMIP5 models: ACCESS1-0, ACCESS1-3, BNU-ESM, CNRM-CM5, CSIRO-Mk3-6-0, CanESM2, GFDL-ESM2M, IPSL-CM5A-LR, IPSL-CM5A-MR, IPSL-CM5B-LR, NorESM1-M, bcc-csm1-1-m.

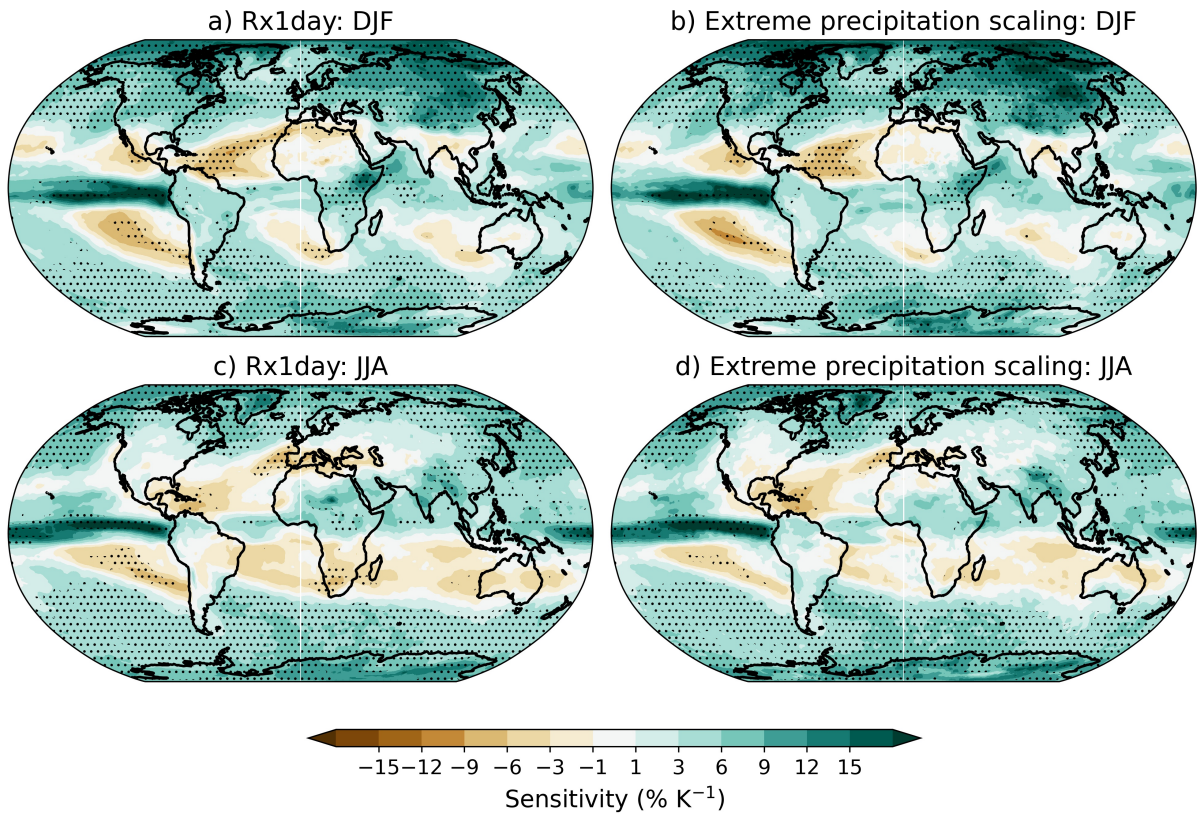


Figure S1. Comparison between CMIP5 multi-model mean changes in seasonal daily maximum precipitation (Rx1day) in DJF (a) and JJA (c) and changes in the corresponding scaling estimate calculated from Eq. 1 in the main text (b, d). Stippling indicates where at least 90% models agree on the sign of the change.

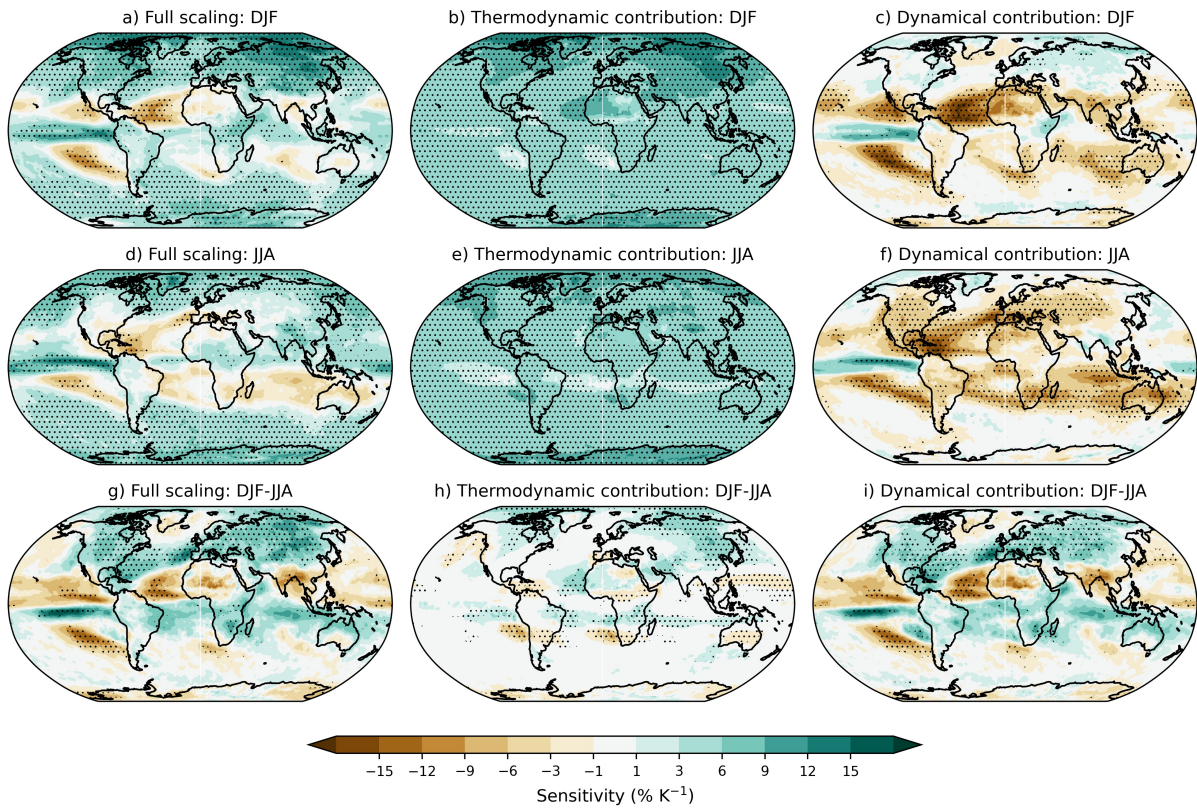


Figure S2. As in Fig. 1 except that the normalization is over the period 1950-2100 instead of 1950-2000. The results are generally similar, except that the difference between the thermodynamic contribution in DJF and JJA is reduced slightly in percentage terms, although this does not remove the amplified thermodynamic sensitivity over Northern Hemisphere land during DJF.

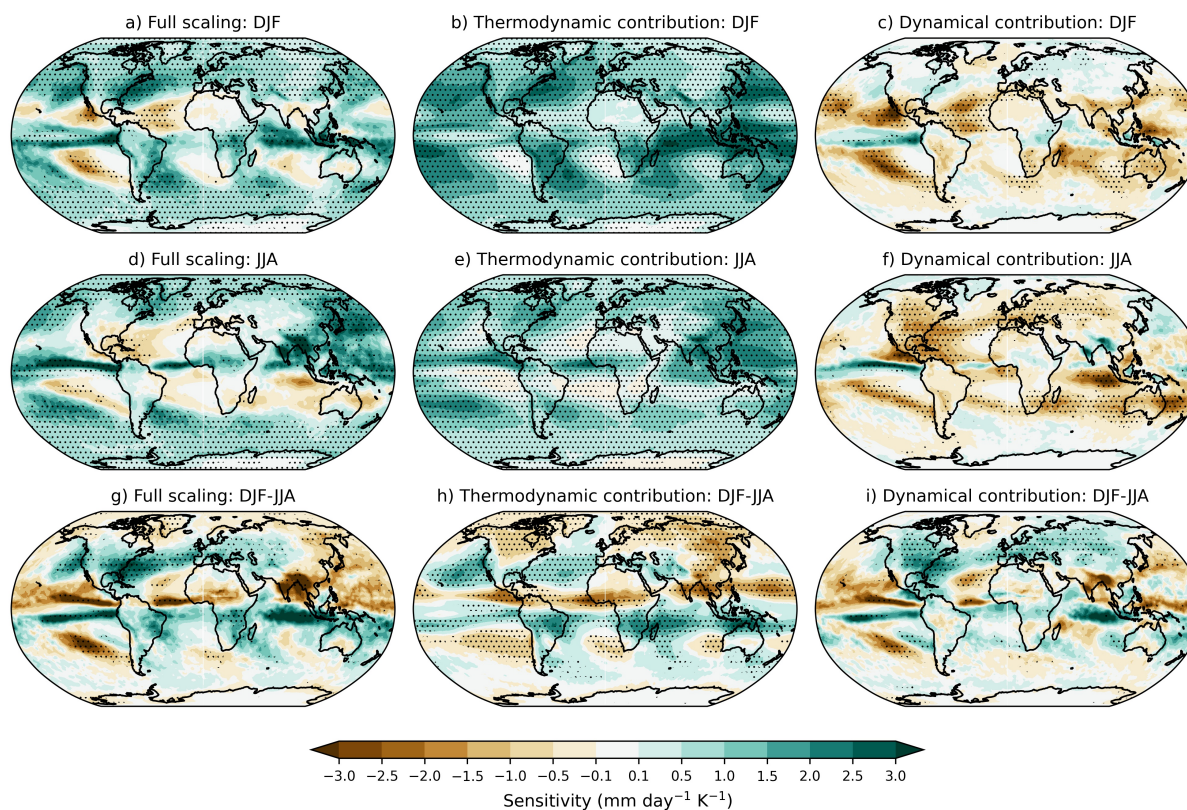


Figure S3. As in Fig. 1 expect that here we do not normalize the daily maximum time-series by their average over the 1950-2000 period, and thus the trends are in $\text{mm day}^{-1} \text{K}^{-1}$ as opposed to $\% \text{K}^{-1}$. There is still a winter-summer contrast in changes in precipitation extremes over much of NH midlatitude land but not to the same extent as when percentage changes are considered.

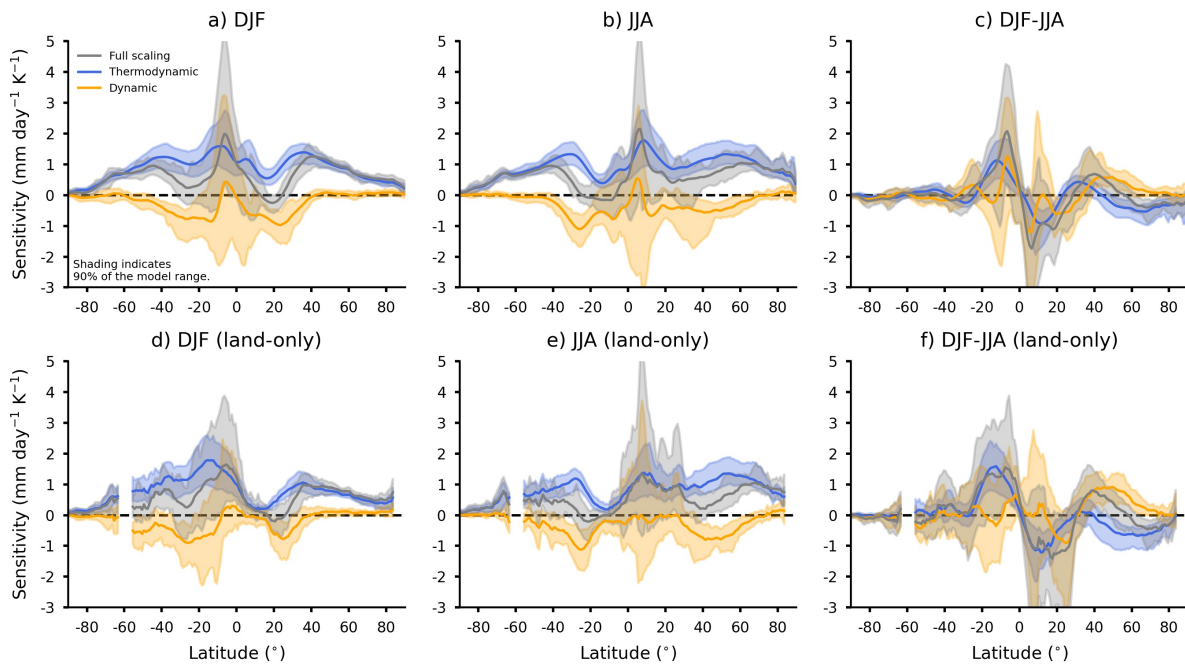


Figure S4. As in Fig. 2 expect that here we do not normalize the daily maximum time-series by their average over the 1950-2000 period, and thus the trends are in mm day⁻¹ K⁻¹ as opposed to % K⁻¹. This figure demonstrates that while the dynamical contribution still contributes to a winter-summer contrast over the NH in absolute terms, it is largely cancelled out in the zonal mean by weaker thermodynamic trends in DJF than in JJA.

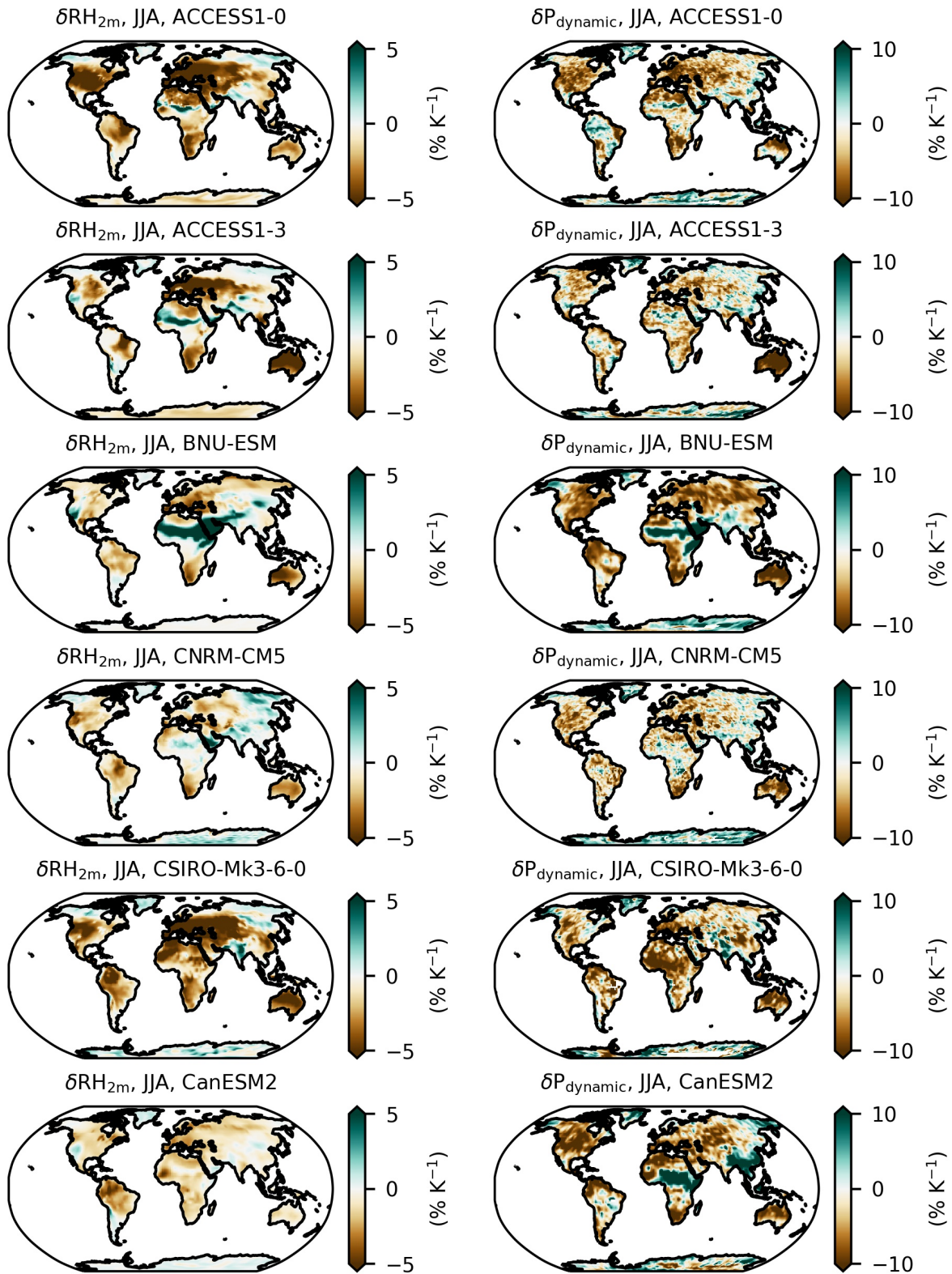


Figure S5. As in Fig.3a,b except showing the first six CMIP5 models individually.

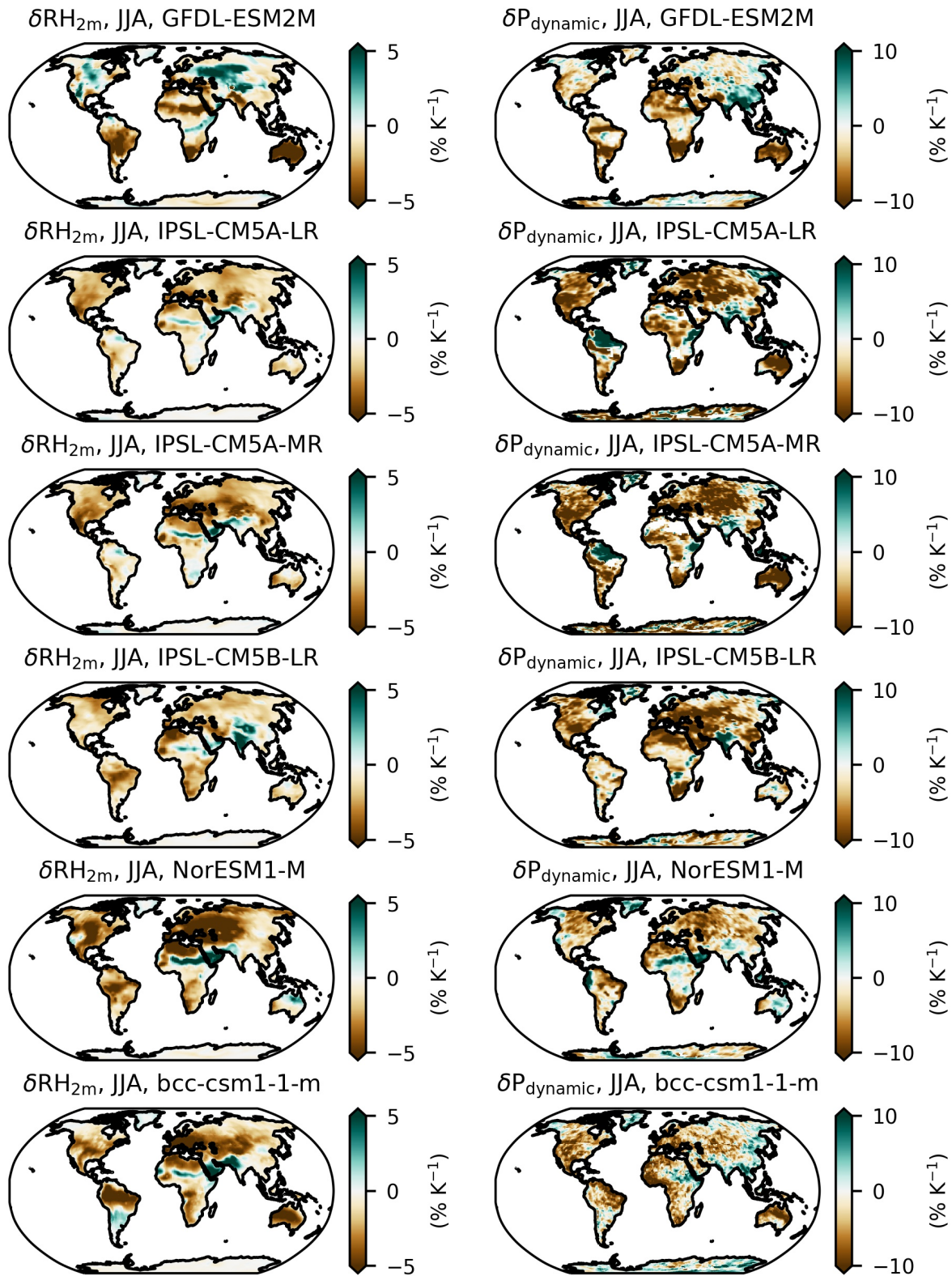


Figure S6. As in Fig.3a,b except showing the last six CMIP5 models individually.

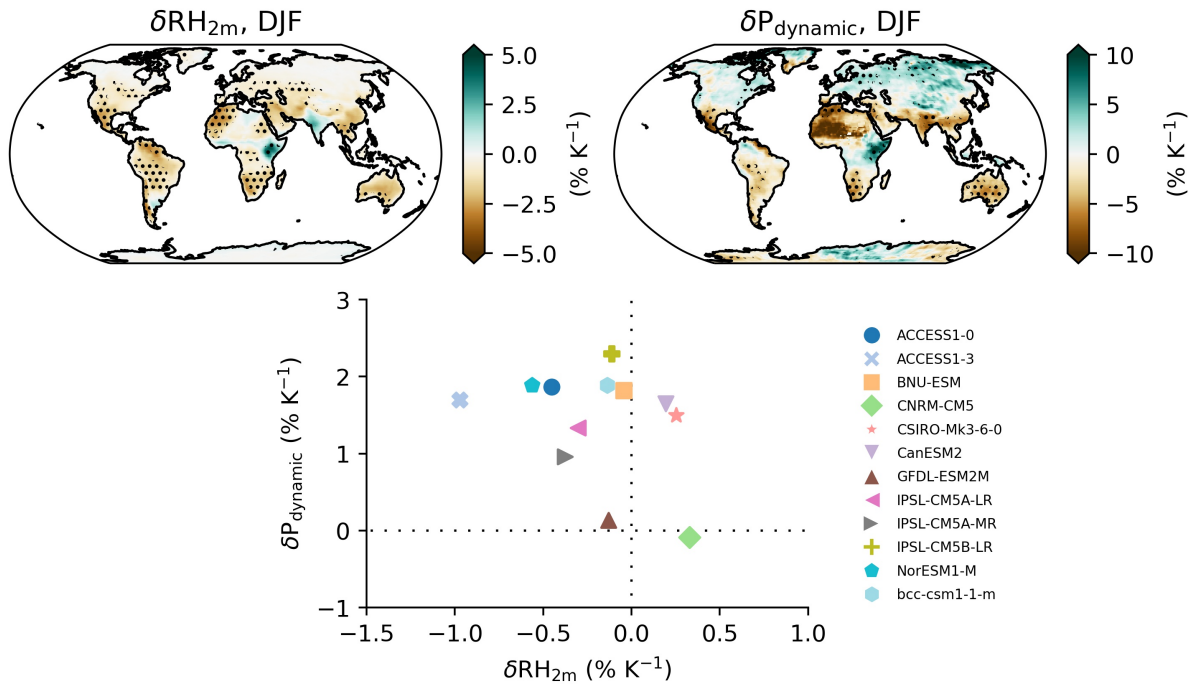


Figure S7. As in Fig. 3, but for DJF. Most models predict a weak decrease in near-surface relative humidity with warming over Northern Hemisphere land in this season, but the dynamical contribution over Northern Hemisphere land is positive in DJF. The lack of a correlation with near-surface relative humidity over the Northern Hemisphere during DJF makes sense given that precipitation extremes during DJF are associated with weather systems that are less strongly influenced by convection than during JJA.

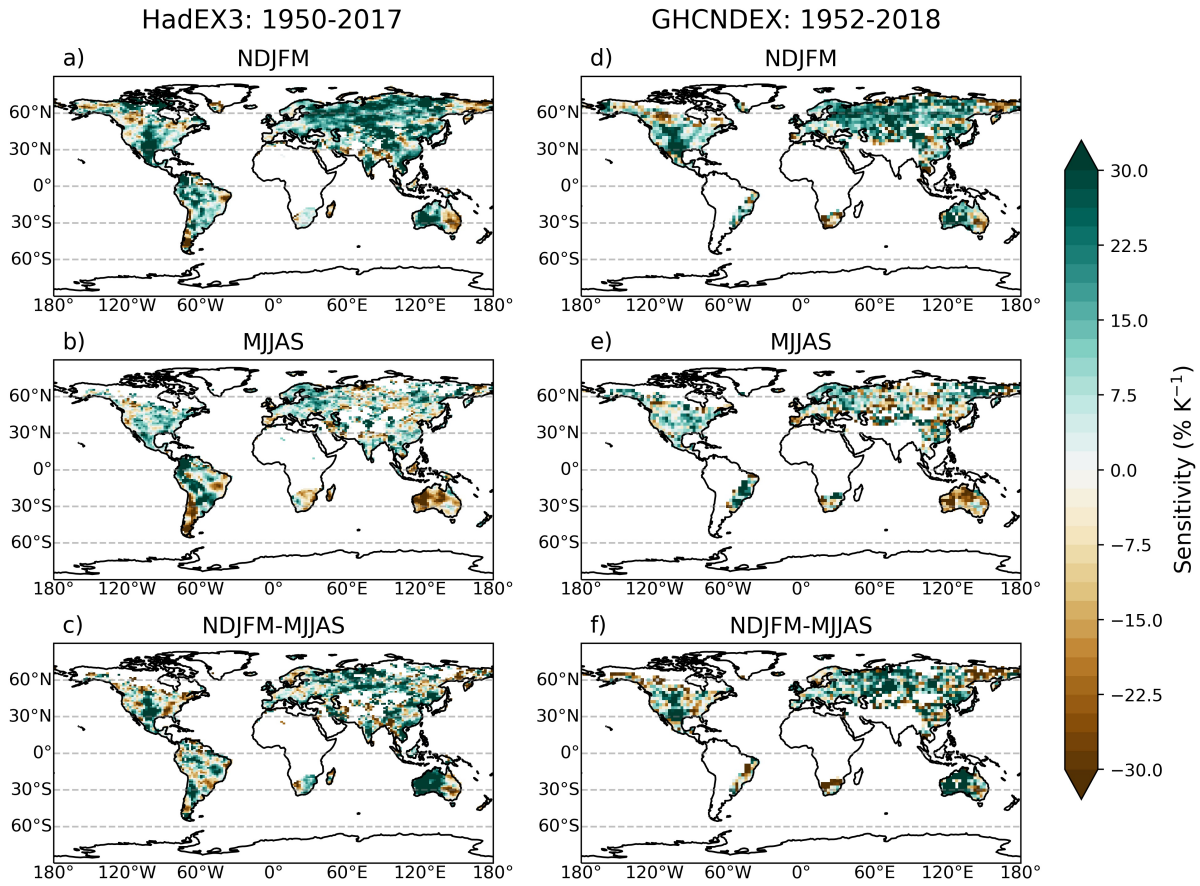


Figure S8. Regional sensitivities of Rx1day to global temperature changes over the period 1950-2017 for HadEX3 (a,b,c) and 1952-2018 for GHCNDEX (d,e,f). Sensitivities are plotted for grid boxes with at least 45 years of data, and for the seasonal contrast we require grid boxes to have at least 45 years with data for both NDJFM and MJJAS (see Section 2 of main text for details). The HadEX3 and GHCNDEX datasets have spatial resolutions of $1.25^\circ \times 1.875^\circ$ and $2.5^\circ \times 2.5^\circ$, respectively. The figure also shows that HadEX3 has substantially more grid boxes in the tropics. Visually it is also apparent that the extreme precipitation sensitivity is higher during NDJFM (a, d) than in MJJAS (b, d) in both datasets over the extratropical Northern Hemisphere, corresponding to a winter-summer contrast over this region (c, f).

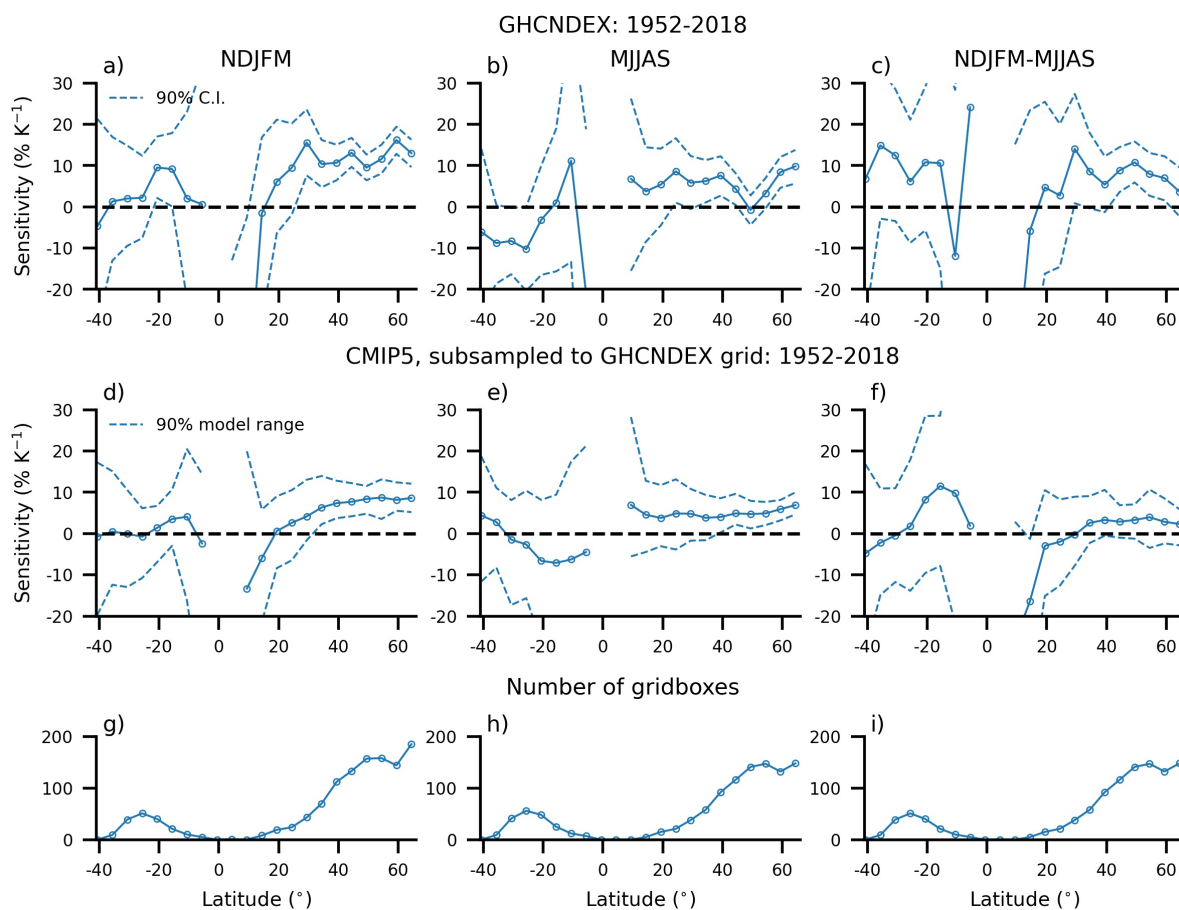


Figure S9. As in Fig. 4, except for the GHCNDEX observational dataset rather than HadEX3. CMIP5 simulations are subsampled to GHCNDEX in making this figure.

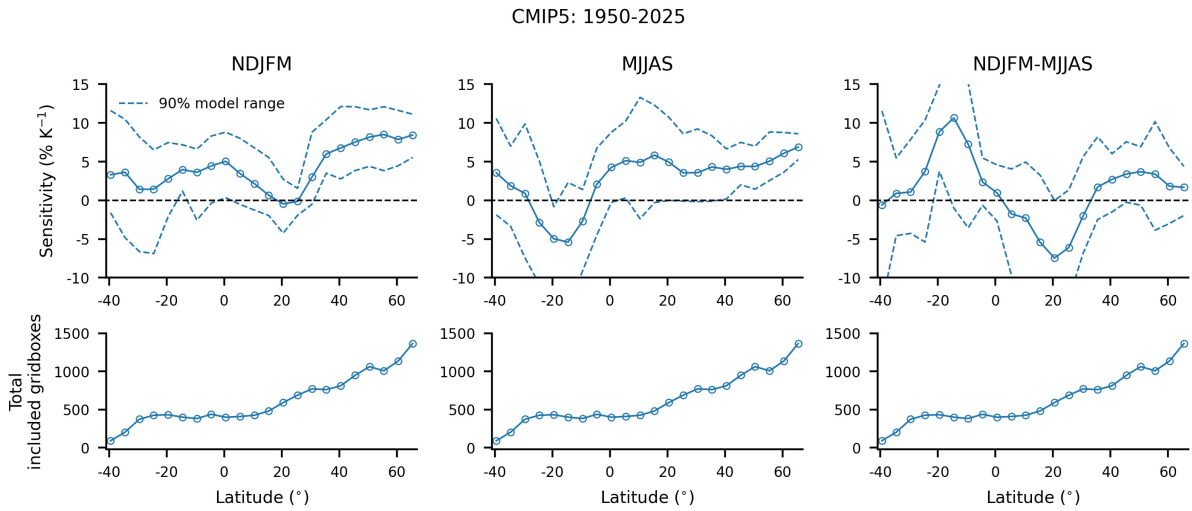


Figure S10. Sensitivity of seasonal precipitation extremes over land to warming in CMIP5 over the period 1950-2025 for NDJFM, MJJAS and NDJFM-MJJAS. The sensitivities are calculated the same as in Fig. 4 and Fig. S9 except for here we do not subsample the CMIP5 models to the spatio-temporal grid of the observations. This shows that the winter-summer contrast is also present in CMIP5 models when there is no missing data. The number of included gridboxes is the same in each season, but there are latitudinal variations which reflect the fact there is less land in some 5° latitude bands than in others.